Robust Gate Driving Vectors to Load Current and Temperature Variations for Digital Gate Drivers

Toru Sai[1], Koutaro Miyazaki[1], Hidemine Obara[2], Tomoyuki Mannen[3], Keiji Wada[3], Ichiro Omura[4], Takayasu Sakurai[1] and Makoto Takamiya[1]

[1]The University of Tokyo, Tokyo, Japan
[2]Yokohama National University, Kanagawa, Japan
[3]Tokyo Metropolitan University, Tokyo, Japan
[4]Kyusyu Institute of Technology, Fukuoka, Japan

sai@iis.u-tokyo.ac.jp

Abstract— A digital gate driver is effective to solve the trade-off between the switching loss and the current/voltage overshoot of power transistors. A load current and temperature dependent optimization of the gate driving vectors for the digital gate drivers, however, is required [13], because an optimum vector at a particular load current and temperature does not often work at different conditions. When sensors for the load current and/or temperature are not available, the digital gate drivers are not useful under load current and temperature variations. To solve the problem, robust gate driving vectors to load current and temperature variations for the digital gate drivers are proposed. To compare a conventional single-step gate drive and the proposed robust gate driving vectors, the switching loss and the current/voltage overshoot in turn-on/off state of IGBT are measured by using a 6-bit programmable digital gate driver IC across nine conditions including different load currents (20 A, 50 A, and 80 A) and temperatures (25 °C, 75 °C, and 125 °C). The performance of the switching loss and the current/voltage overshoot of the proposed robust vectors is improved by 2% to 11 % and 16 % to 29 % across the nine conditions in turn-on/off state, respectively, which indicates that the proposed robust vectors requiring no current and temperature sensors are a useful method for the digital gate drivers.

Keywords—Gate driver, IGBT, Load current, Temperature

I. INTRODUCTION

Active gate driving of power transistors, where the gate driving current is dynamically controlled during the turn-on/off transients, is a promising technology to solve the trade-off between the switching loss (E_{LOSS}) and the current overshoot ($I_{OVERSHOOT}$) or voltage overshoot ($V_{OVERSHOOT}$) of power transistors with a conventional fixed gate resistance driver. Digital gate drivers [1-13] are useful for the active gate driving, because the gate driving current is programmable with gate driving vectors using a software. For example, a 6-bit programmable digital gate driver with four 6-bit variables, where an optimum gate driving vector is automatically found out of 64^4 (~1.7 x 10^7) combinations using a simulated annealing algorithm, reduces E_{LOSS} by 55% at the same $V_{OVERSHOOT}$ and reduces $V_{OVERSHOOT}$ by 53% at the same E_{LOSS} at the turn-off of IGBT [5]. The optimum gate driving vector, however, changes depending on a load current (I_{LOAD}) and temperature [13]. When an optimum vector at a particular I_{LOAD} and temperature is reused to another I_{LOAD} and temperature, E_{LOSS} and $I_{OVERSHOOT}/V_{OVERSHOOT}$ are sometimes worse than the conventional single-step gate drive [13]. Therefore, I_{LOAD} and temperature dependent gate driving vectors are required [13]. When sensors for I_{LOAD} and/or

temperature are not available, the digital gate drivers are not useful under load current and temperature variations. To solve the problem, robust gate driving vectors to I_{LOAD} and temperature variations for the digital gate drivers are proposed in this paper. Compared with the conventional single-step gate drive, the digital gate driver has a potential to reduce E_{LOSS} and $I_{OVERSHOOT}/V_{OVERSHOOT}$, because the digital gate driver with four variables has a higher flexibility than the conventional single-step gate drive with only one variable. E_{LOSS} and $I_{OVERSHOOT}/V_{OVERSHOOT}$ in turn-on/off state of IGBT are measured by using a 6-bit programmable digital gate driver IC across nine conditions including different load currents (20 A, 50 A, and 80 A) and temperatures (25 °C, 75 °C, and 125 °C). Compared with the conventional single-step gate drive, E_{LOSS} and $I_{OVERSHOOT}/V_{OVERSHOOT}$ of the digital gate drivers with the proposed robust vectors is reduced across the nine conditions.

II. MEASUREMENT SETUP

Fig. 1 shows a circuit schematic of the measurement setup for the double pulse test for turn-on and turn-off of IGBT at 300 V. The measurement system including a 6-bit programmable digital gate driver, 2-in-1 IGBT module (2MBI100VA-060-50, 600 V, 100 A), and the signal acquisition/control system is the same as [13] except for the gate driving vectors. In order to realize a programmable 63-level drivability in the programmable gate driver, 63 parallel transistors are connected to the gate of IGBT and a 6-bit control signal is applied to specify the number of activated PMOS (NMOS) transistors, n_{PMOS} (n_{NMOS}) [6]. Fig. 2 (a) shows the gate driving vectors and waveforms in the 6-bit digital gate driver. In this paper, the gate driving vector is
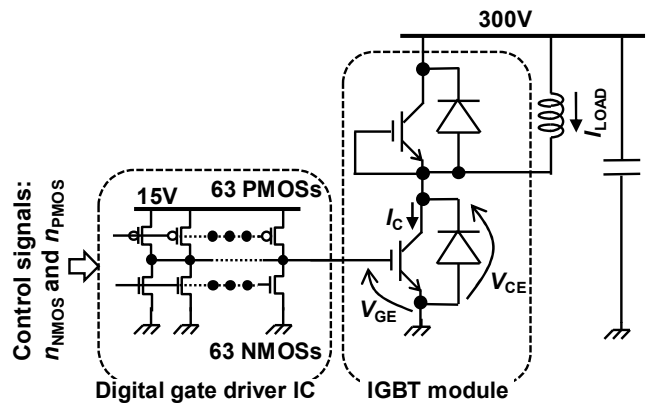

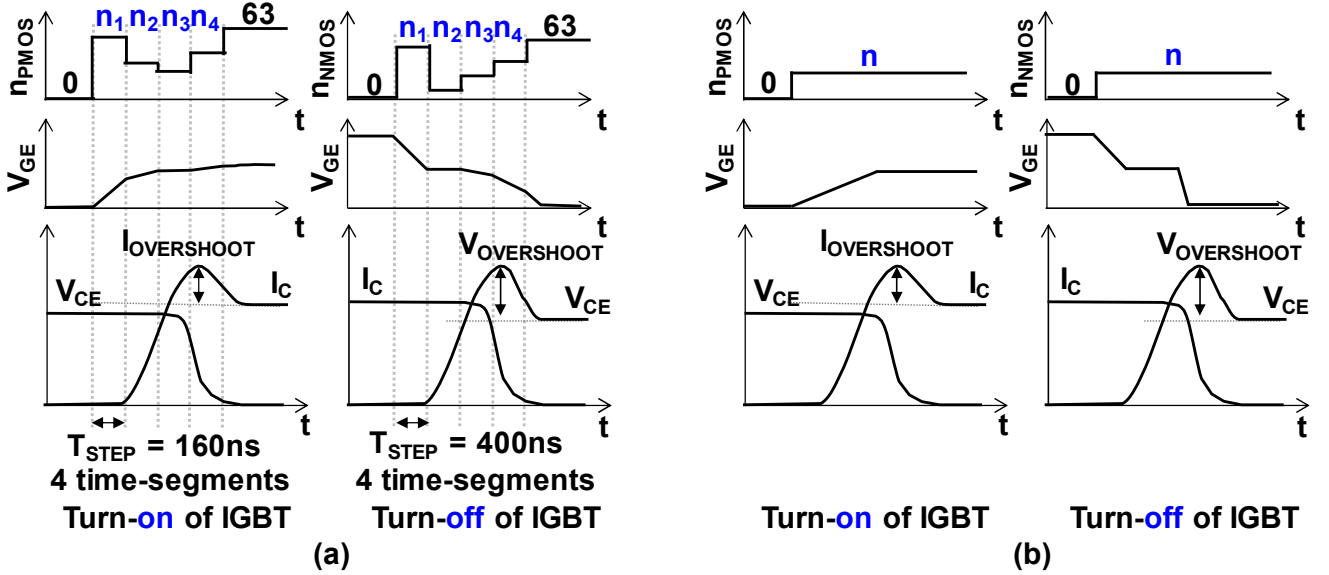Fig. 1. Circuit schematic of measurement setup.

Fig. 2. Gate driving vectors and waveforms. (a) Proposed. (b) Conventional single-step gate drive.
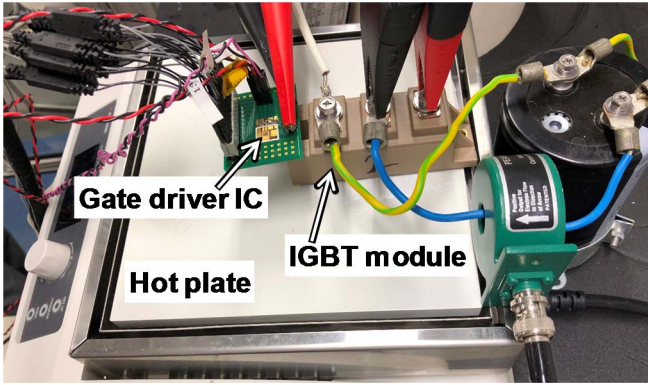

Fig. 3. Photo of measurement setup.

defined as (n_1, n_2, n_3, n_4), where n_1, n_2, n_3, and n_4 are integers from 0 to 63. Four 160-ns time steps in turn-on state and four 400-ns steps in turn-off state are used. Fig. 2 (b) shows the gate driving vectors and waveforms of the conventional single-step gate drive emulated by the digital gate driver. The

gate driving vector is (n), where n is an integer from 0 to 63. Fig. 3 shows the photo of the measurement setup. The IGBT module is put on a hot plate to control the temperature, while the gate driver IC is away from the hot plate.

III. How to Find Robust Gate Driving Vectors

In this chapter, a method to find the proposed robust gate driving vectors is explained. First, E_{LOSS} and $I_{OVERSHOOT}/V_{OVERSHOOT}$ in turn-on/off state of IGBT are measured by using the 6-bit digital gate driver IC with all combinations of four variables at the nine conditions, $(I_{LOAD},$ temperature) = (20 A, 25 °C), (20 A, 75 °C), (20 A, 125 °C), (50 A, 25 °C), (50 A, 75 °C), (50 A, 125 °C), (80 A, 25 °C), (80 A, 75 °C), and (80 A, 125 °C). The levels of n_1, n_2, n_3, and n_4 are reduced from 64 to 10, because the number of combinations of 64^4 (~1.7 x 10^7) is too large to measure. Specifically, in this paper, n_1, n_2, n_3, and n_4 are 0, 7, 14, 21, 28, 35, 42, 49, 56, and 63, and the number of combinations is 10^4. The required time for 10^4 measurements is 36 minutes. In

TABLE I. Top five ranking of f_{OBJ_ON} out of 10^4 measurements in turn-on state. Proposed robust gate driving vector is $(n_1, n_2, n_3, n_4) =$ (7, 35, 7, 14).

| Rank | Vectors | | | | f_{OBJ} | | | | | | | | | Min. f_{OBJ} |
| | | | | | 25℃ | | | 75℃ | | | 125℃ | | | |
	n_1	n_2	n_3	n_4	(1) 20A	(2) 50A	(3) 80A	(4) 20A	(5) 50A	(6) 80A	(7) 20A	(8) 50A	(9) 80A	in (1) to (9)
1	7	35	7	14	6.106E-01	6.133E-01	5.887E-01	6.568E-01	6.591E-01	6.369E-01	6.835E-01	6.961E-01	6.983E-01	6.983E-01
2	49	7	14	42	6.541E-01	5.983E-01	5.859E-01	6.813E-01	6.491E-01	6.236E-01	6.987E-01	6.925E-01	6.777E-01	6.987E-01
3	49	7	14	28	6.598E-01	6.173E-01	5.919E-01	6.840E-01	6.462E-01	6.343E-01	6.981E-01	7.015E-01	6.789E-01	7.015E-01
4	49	7	14	35	6.650E-01	6.148E-01	5.881E-01	6.830E-01	6.417E-01	6.286E-01	7.016E-01	6.896E-01	6.848E-01	7.016E-01
5	49	7	14	56	6.658E-01	5.976E-01	5.849E-01	6.857E-01	6.326E-01	6.202E-01	7.016E-01	6.895E-01	6.802E-01	7.016E-01

TABLE II. Top five ranking of f_{OBJ_OFF} out of 10^4 measurements in turn-off state. Proposed robust gate driving vector is $(n_1, n_2, n_3, n_4) =$ (49, 42, 7, 14).

| Rank | Vectors | | | | f_{OBJ} | | | | | | | | | Min. f_{OBJ} |
| | | | | | 25℃ | | | 75℃ | | | 125℃ | | | |
	n_1	n_2	n_3	n_4	(1) 20A	(2) 50A	(3) 80A	(4) 20A	(5) 50A	(6) 80A	(7) 20A	(8) 50A	(9) 80A	in (1) to (9)
1	49	42	7	14	7.147E-01	5.348E-01	5.403E-01	7.566E-01	5.978E-01	5.884E-01	7.396E-01	6.700E-01	6.637E-01	7.566E-01
2	49	42	7	56	7.389E-01	5.429E-01	5.469E-01	7.540E-01	6.001E-01	5.943E-01	7.609E-01	6.853E-01	6.643E-01	7.609E-01
3	49	42	7	7	7.166E-01	5.384E-01	5.426E-01	7.551E-01	5.892E-01	5.917E-01	7.651E-01	6.838E-01	6.594E-01	7.651E-01
4	49	42	7	42	7.137E-01	5.308E-01	5.438E-01	7.549E-01	6.134E-01	5.892E-01	7.657E-01	6.779E-01	6.650E-01	7.657E-01
5	49	42	7	63	7.370E-01	5.376E-01	5.532E-01	7.538E-01	5.913E-01	5.955E-01	7.666E-01	6.747E-01	6.642E-01	7.666E-01
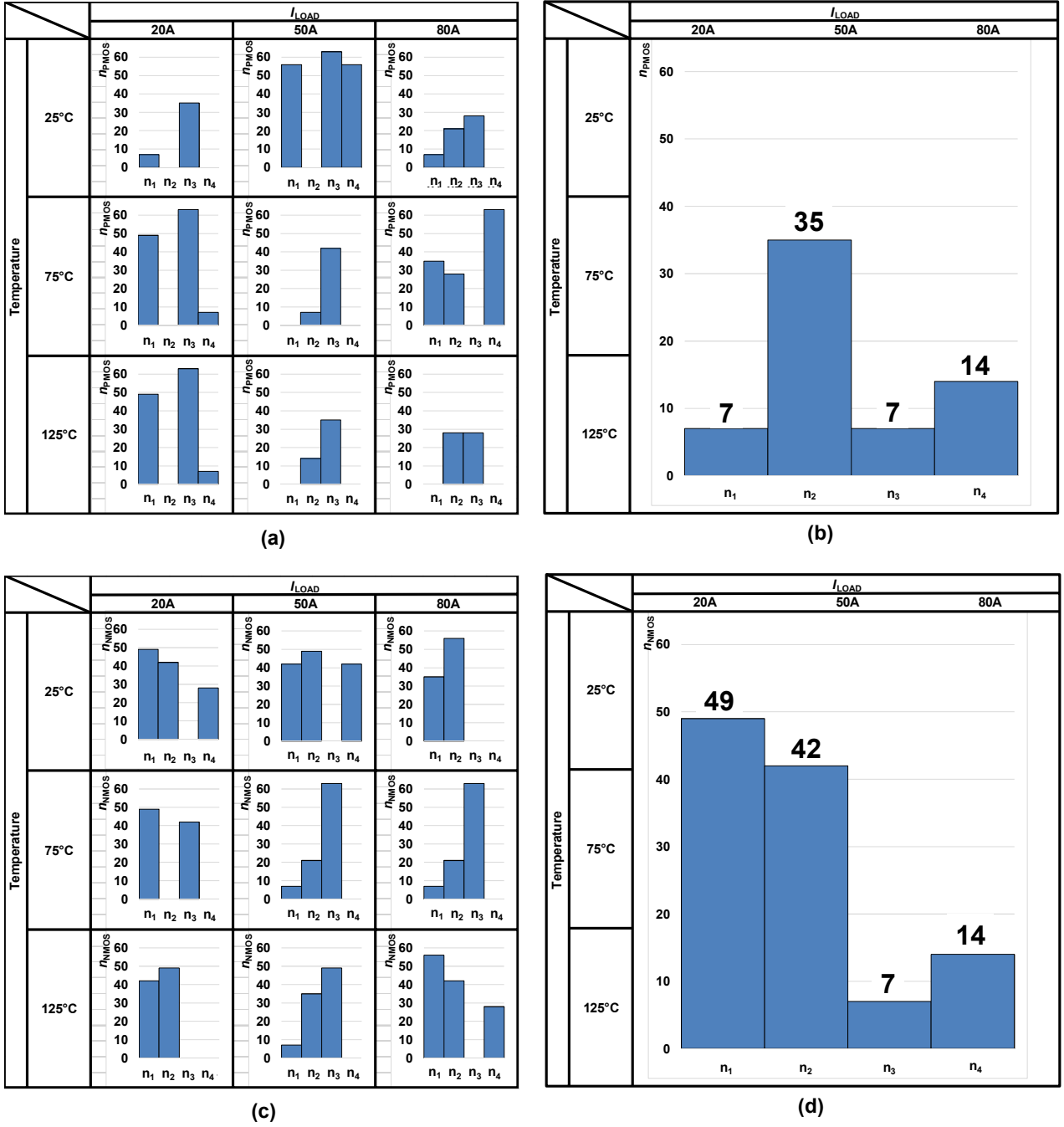
Fig. 4. Gate driving vectors across nine conditions including different I_{LOAD} (20 A, 50 A, and 80 A) and temperatures (25 °C, 75 °C, and 125 °C). (a) and (b) Turn-on. (c) and (d) Turn-off. (a) and (c) Best gate driving vectors at each I_{LOAD} and temperature. (b) and (d) Proposed robust gate driving vectors.

total, the measurement time across the nine conditions is 5.5 hours for 9 x 10^4 measurements. Then, the turn-on object function (f_{OBJ_ON}) and the turn-off object function (f_{OBJ_OFF}) of each measurement are calculated to evaluate E_{LOSS} and $I_{OVERSHOOT}/V_{OVERSHOOT}$.

$$f_{OBJ\_ON} = \sqrt{\left(\frac{E_{LOSS}}{E_{LOSS,MAX}}\right)^2 + \left(\frac{I_{OVERSHOOT}}{I_{OVERSHOOT,MAX}}\right)^2} \quad (1)$$

$$f_{OBJ\_OFF} = \sqrt{\left(\frac{E_{LOSS}}{E_{LOSS,MAX}}\right)^2 + \left(\frac{V_{OVERSHOOT}}{V_{OVERSHOOT,MAX}}\right)^2} \quad (2)$$

where the subscript MAX signifies the maximum of the corresponding quantity. Small f_{OBJ} is preferred. Tables I and II show the top five ranking of f_{OBJ_ON} and f_{OBJ_OFF} out of 10^4 measurements, respectively. Maximum f_{OBJ} in each vector across the nine conditions are selected and are arranged in ascending order. The top ones in Tables I and II are the proposed robust gate driving vectors, where (n_1, n_2, n_3, n_4) = (7, 35, 7, 14) in turn-on state and (n_1, n_2, n_3, n_4) = (49, 42, 7, 14) in turn-off state. The proposed robust gate driving vectors achieve the best f_{OBJ}'s out of the 10^4 worst f_{OBJ}'s across the nine conditions, which is the reason why the proposed vectors are robust to I_{LOAD} and temperature variations.
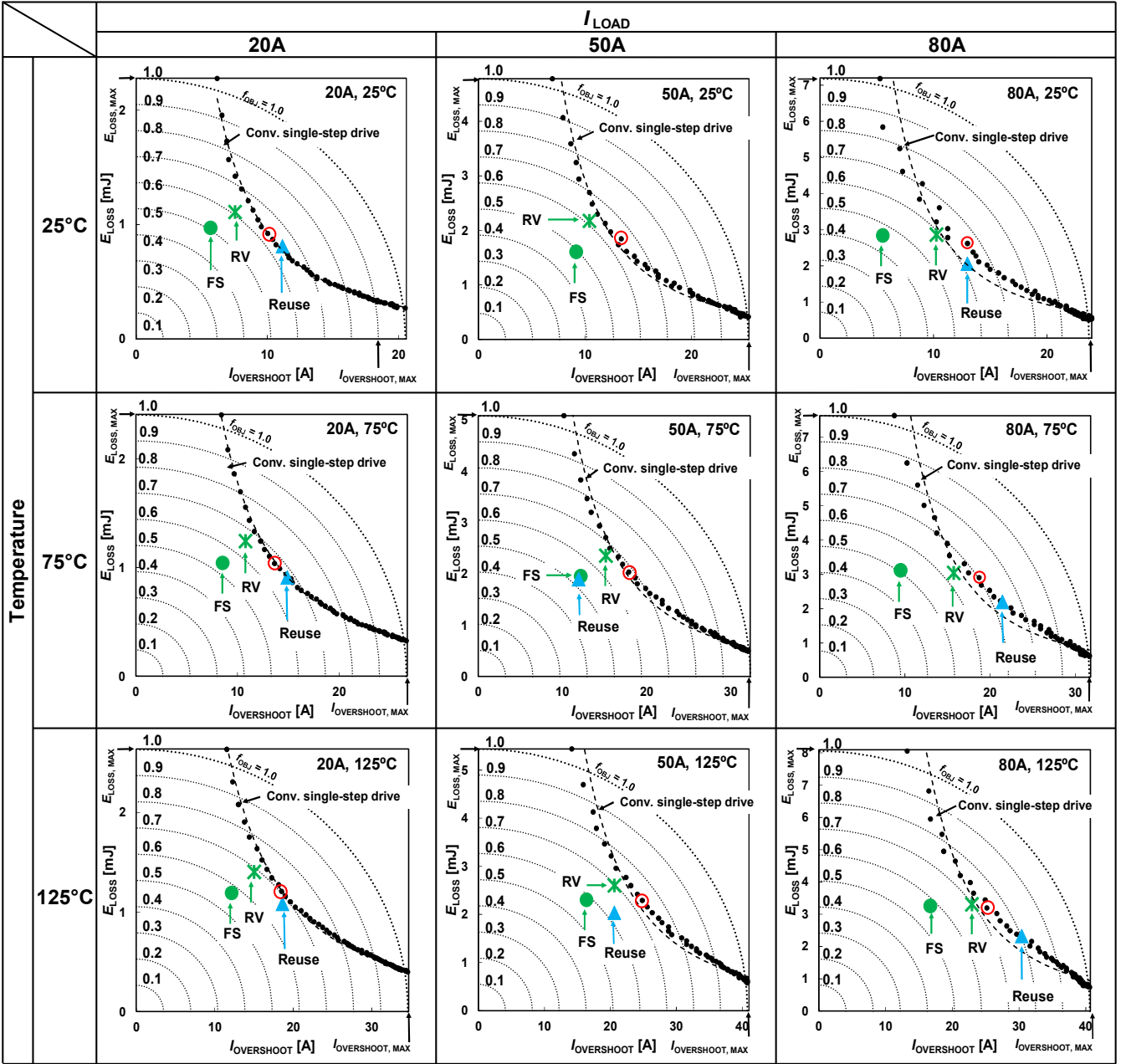
Fig. 5. Measured E_{LOSS} vs. $I_{OVERSHOOT}$ of four gate drives in turn-on state. Black curves: trade-off curves of conventional single-step gate drive with varied n. Red circles: Representative points of conventional single-step gate drive. Green asterisks: proposed robust vectors (RV). Green circles: full search (FS). Blue triangles: reuse of optimum gate driving vectors at 50 A, 25 °C.

IV. MEASURED RESULTS

In order to clarify the advantage of the proposed robust gate driving vectors, E_{LOSS} and $I_{OVERSHOOT}/V_{OVERSHOOT}$ of four gate drives are compared in measurements across the nine conditions including different I_{LOAD} (20 A, 50 A, and 80 A) and temperatures (25 °C, 75 °C, and 125 °C). Figs. 4 (a) and (c) show the best gate driving vectors achieving the minimum f_{OBJ}'s in 10^4 measurements at each I_{LOAD} and temperature in turn-on and turn-off state, respectively. In this paper, they are defined as "full search (FS)" and the FS shows the lower limit of f_{OBJ} at each I_{LOAD} and temperature. Figs. 4 (b) and (d) show the proposed robust gate driving vectors (RV) extracted from Tables I and II in turn-on and turn-off state, respectively. In RV, different from FS, the same vector is applied to the nine conditions. Fig. 5 shows the measured E_{LOSS} vs. $I_{OVERSHOOT}$ of

the four gate drives in turn-on state. Fig. 6 shows the measured E_{LOSS} vs. $V_{OVERSHOOT}$ of the four gate drives in turn-off state. The black curves show the trade-off curves of the conventional single-step gate drive in Fig. 2 (b) with varied n from 5 to 63. The red circles show the representative points of the conventional single-step gate drive, where $n = 15$ in turn-on state and $n = 9$ in turn-off state. The green asterisks show the proposed RV. The green circles show FS, which means the lower limit of f_{OBJ} at each I_{LOAD} and temperature. The blue triangles show the reuse of the optimum gate driving vectors at (50 A, 25 °C) [13] for comparison, which is defined as "Reuse". The dotted concentric curves Figs. 5 and 6 show the contour of f_{OBJ_ON} and f_{OBJ_OFF} defined in Eqs. (1) and (2), respectively. Figs. 7 (a) and (b) show f_{OBJ} of the four gate drives at the nine conditions in turn-on and turn-off state, respectively. The red circles in Figs. 5 and 6 are plotted in Fig.
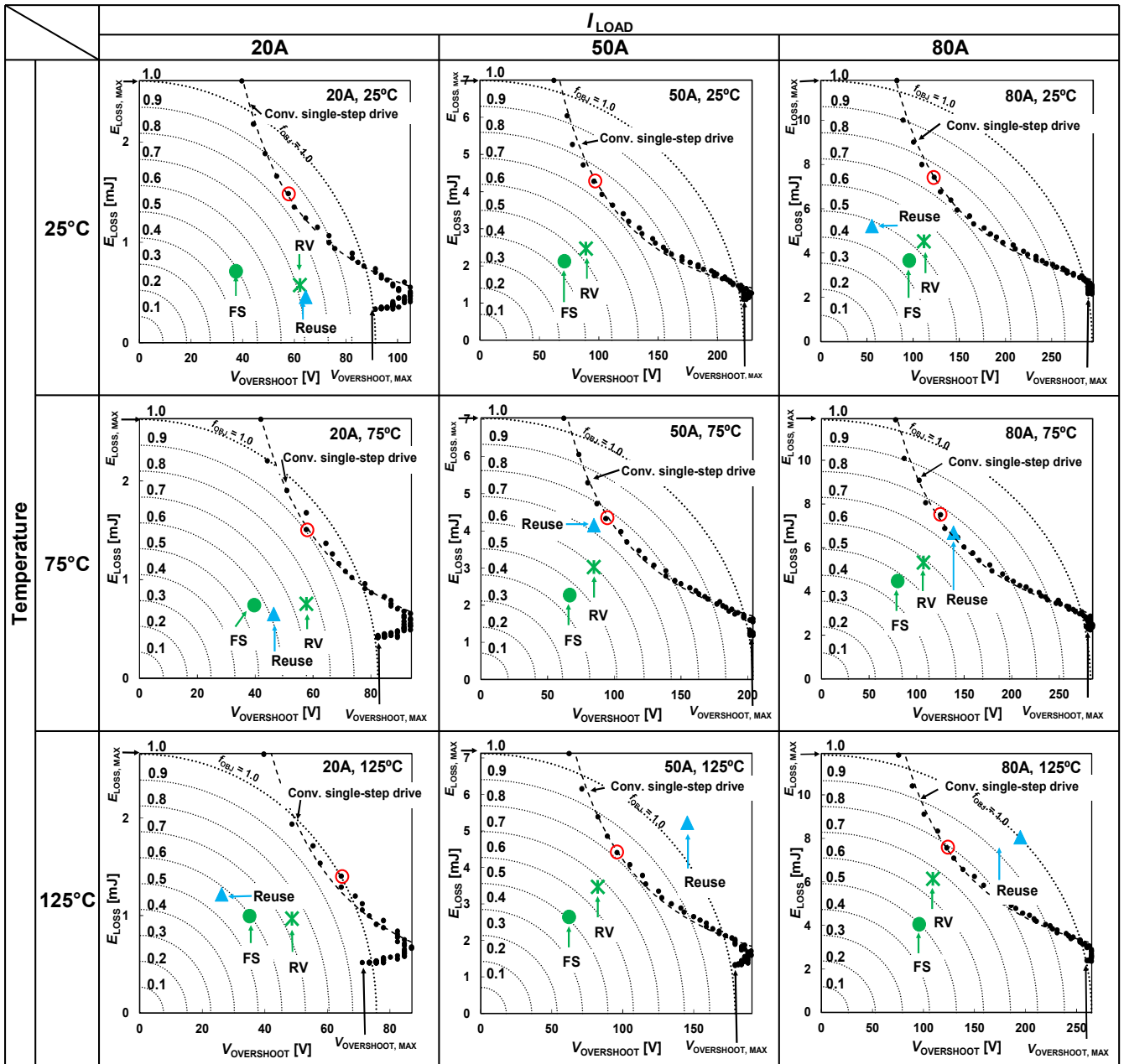
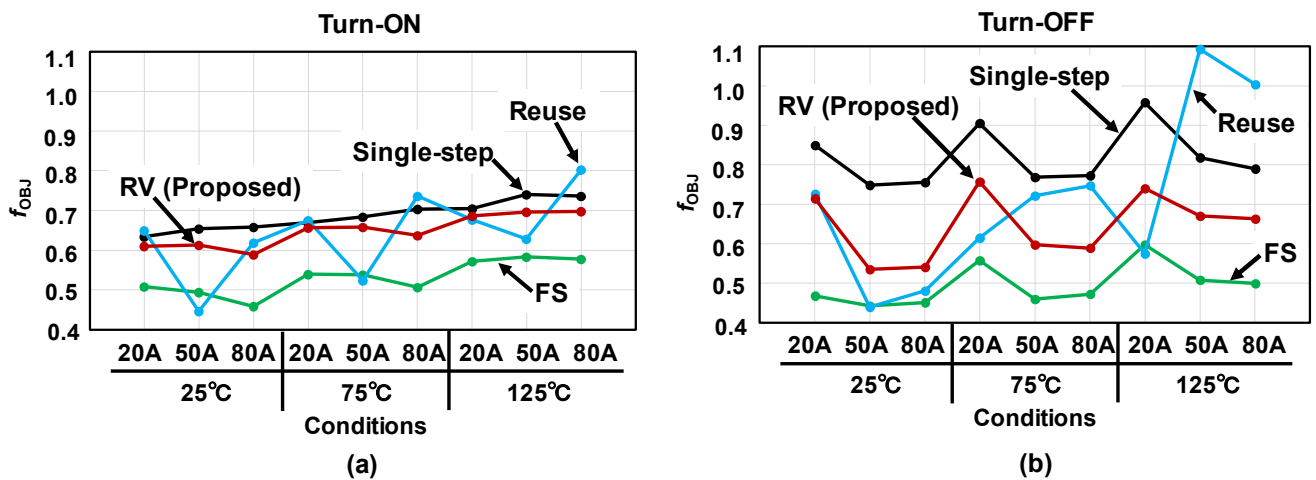Fig. 6. Measured E_{LOSS} vs. $V_{OVERSHOOT}$ of four gate drives in turn-off state.

Fig. 7. f_{OBJ} of four gate drives at the nine conditions. (a) Turn-on. (b) Turn-off.
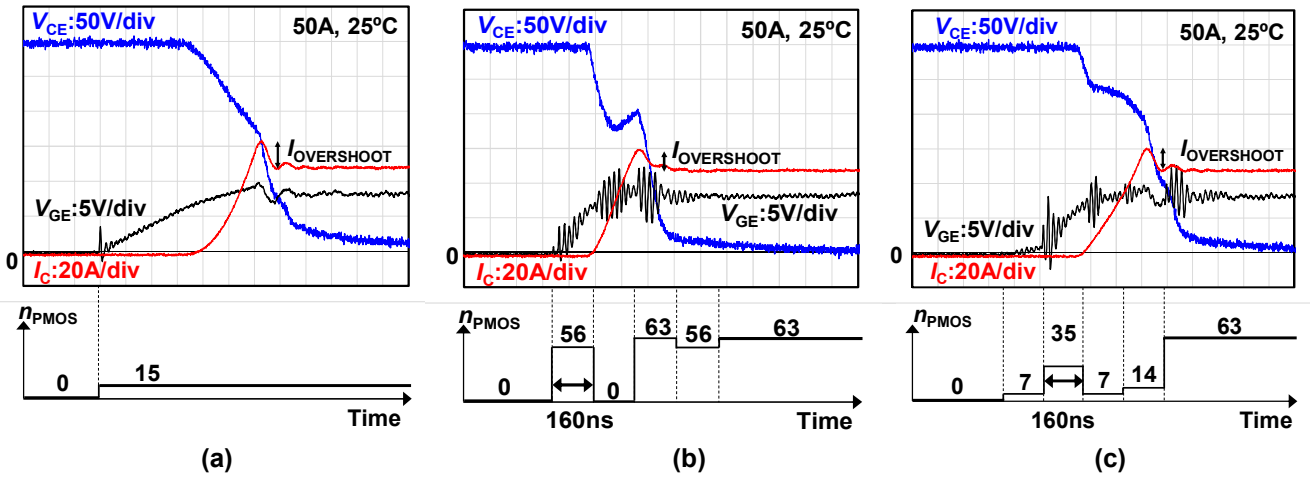
Fig. 8. Gate driving vectors and measured waveforms at 50 A, 25 °C in turn-on. (a) Conventional single-step gate drive. (b) Full search (FS). (c) Proposed robust vectors.
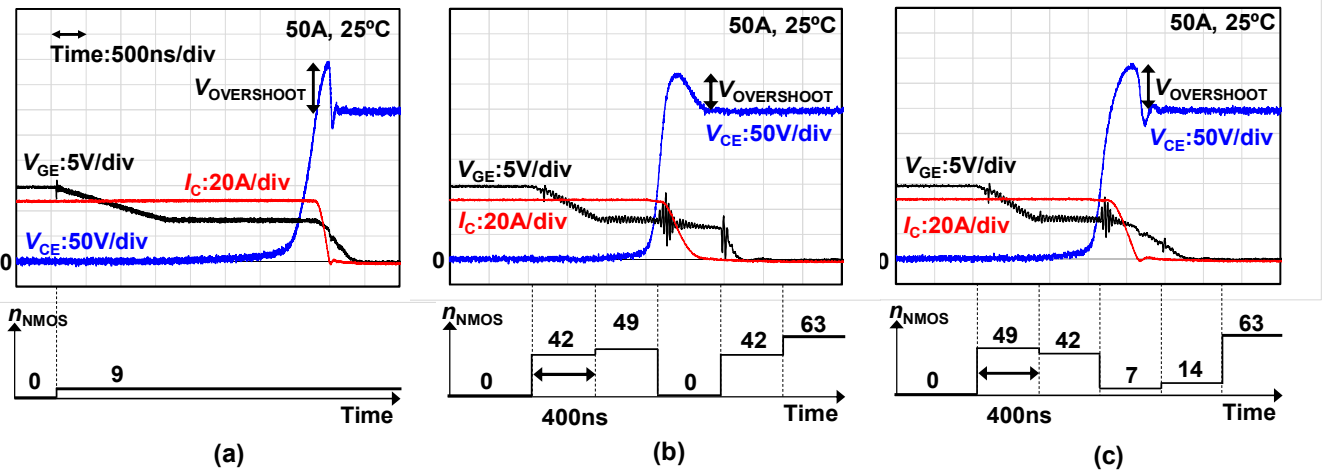

Fig. 9. Gate driving vectors and measured waveforms at 50 A, 25 °C in turn-off. (a) Conventional single-step gate drive. (b) Full search (FS). (c) Proposed robust vectors.
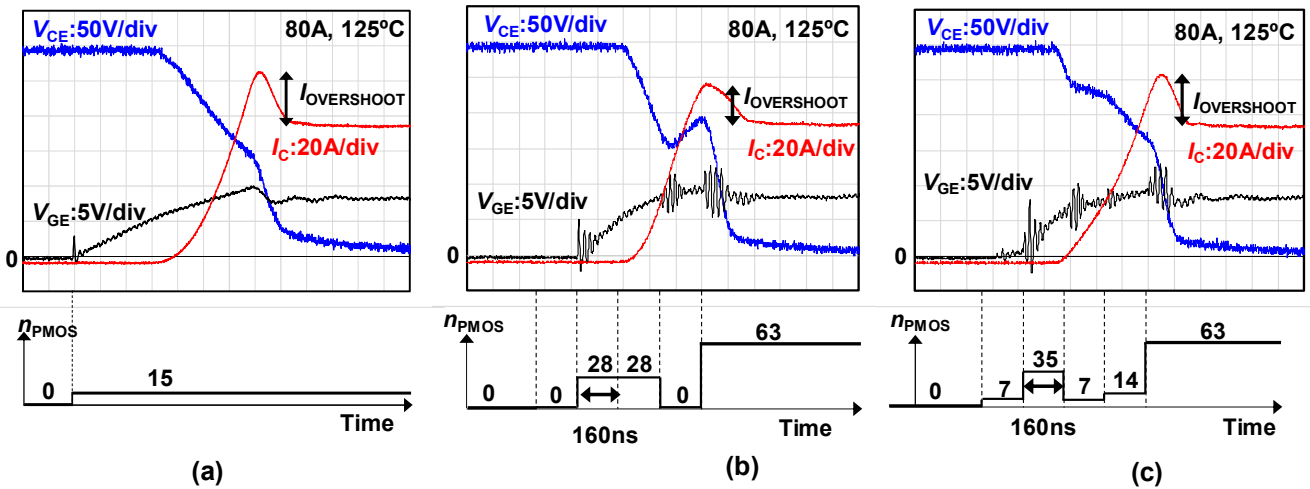

Fig. 10. Gate driving vectors and measured waveforms at 80 A, 125 °C in turn-on. (a) Conventional single-step gate drive. (b) Full search (FS). (c) Proposed robust vectors.

7. As clearly shown in Figs. 5 to 7, f_{OBJ} of the proposed RV is always smaller than that of the conventional single-step gate drive, while f_{OBJ} of Reuse is sometimes larger than that of the conventional single-step gate drive. Therefore, Reuse is not robust to I_{LOAD} and temperature variations, while the proposed RV is robust to I_{LOAD} and temperature variations. Quantitatively, as shown in Fig. 7, f_{OBJ} of the proposed RV is smaller than that of the conventional single-step gate drive by 2 % to 11 % and 16 % to 29 % across the nine conditions in turn-on and turn-off state, respectively. f_{OBJ} of FS is the smallest, while the gate driving vectors are varied depending on I_{LOAD} and temperature as shown in Figs. 4 (a) and (c). The variable vectors depending on I_{LOAD} and temperature do not
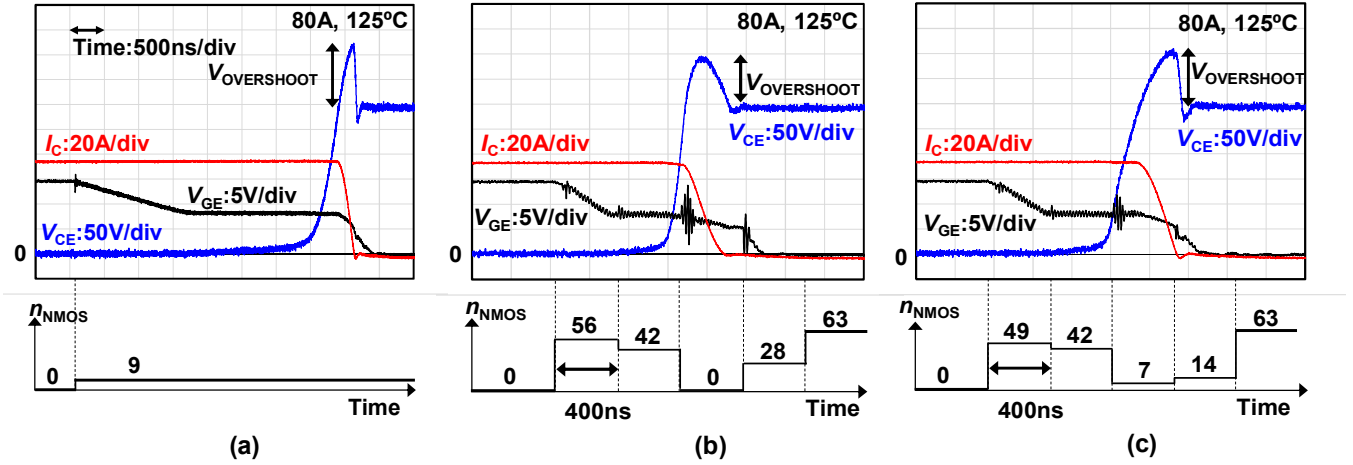
Fig. 11. Gate driving vectors and measured waveforms at 80 A, 125 °C in turn-off. (a) Conventional single-step gate drive. (b) Full search (FS). (c) Proposed robust vectors.

work, when the sensors for I_{LOAD} and/or temperature are not available.

In the followings, the measured waveforms at (50 A, 25 °C) and (80 A, 125 °C) are shown. Figs. 8 (a), (b), and (c) show the gate driving vectors and measured waveforms of the conventional single-step gate drive, FS, and the proposed RV at 50 A, 25 °C in turn-on state, respectively. The corresponding E_{LOSS} and $I_{OVERSHOOT}$ are shown in Fig. 5. $n_2 = 0$ of FS in Fig. 8 (b) and $(n_3, n_4) = (7, 14)$ of RV in Fig. 8 (c) are important to reduce $I_{OVERSHOOT}$, because small gate current before the peak reverse recovery current of the diode is required to reduce $I_{OVERSHOOT}$. Figs. 9 (a), (b), and (c) show the gate driving vectors and measured waveforms of the conventional single-step gate drive, FS, and the proposed RV at 50 A, 25 °C in turn-off state, respectively. The corresponding E_{LOSS} and $V_{OVERSHOOT}$ are shown in Fig. 6. $n_3 = 0$ of FS in Fig. 9 (b) and $n_3 = 7$ of RV in Fig. 9 (c) are important to reduce $V_{OVERSHOOT}$, because small gate current is required to reduce the slew rate of the collector current (I_C). Figs. 10 and 11 show the gate driving vectors and measured waveforms at 80 A, 125 °C in turn-on and turn-off state, respectively. Compared with Figs. 8 and 9, E_{LOSS} and $I_{OVERSHOOT}/V_{OVERSHOOT}$ are increased, because I_{LOAD} is increased from 50 A to 80 A. The tendency of the gate driving vectors of FS and RV, however, is similar to Figs. 8 and 9.

V. CONCLUSIONS

In this paper, the robust gate driving vectors to I_{LOAD} and temperature variations for the 6-bit digital gate drivers are proposed. In the switching measurements of IGBT at 300 V across the nine conditions including different I_{LOAD} (20 A, 50 A, and 80 A) and temperatures (25 °C, 75 °C, and 125 °C), f_{OBJ} of the proposed robust vectors is smaller than that of the conventional single-step gate drive by 2 % to 11 % and 16 % to 29 % in turn-on and turn-off state, respectively. Therefore, the proposed robust vectors requiring no current and temperature sensors are a useful method for the digital gate drivers. A future challenge of the proposed robust vectors is the test cost to find the robust vectors, because 9 x 10^4 measurements take more than 5.5 hours in this work.

REFERENCES

[1] H. Kuhn, T. Koneke, and A. Mertens, "Considerations for a digital gate unit in high power applications," in Proc. IEEE Power Electron. Spec. Conference, Jun. 2008, pp. 2784-2790.

[2] L. Dang, H. Kuhn, and A.Mertens, "Digital adaptive driving strategies for high-voltage IGBTs," in Proc. IEEE Energy Conversion Congress and Exposition, Sep. 2011, pp. 2993–2999.

[3] I. Baraia, J. A. Barrena, G. Abad, J. M. C. Segade, and U. Iraola "An experimentally verified active gate control method for the series connection of IGBT/Diodes," IEEE Trans. on Power Electorinics, vol. 27, issue 2, pp. 1025-1038, Feb. 2012.

[4] M. Blank, T. Glück, A. Kugi, and H.-P. Kreuter, "Slew rate control strategies for smart power ICs based on iterative learning control," in Proc. IEEE Appl. Power Electron. Conf. Expo., Mar. 2014, pp. 2860-2866.

[5] M. Takamiya, K. Miyazaki, H. Obara, T. Sai, K. Wada, and T. Sakurai, "Power electronics 2.0: IoT-connected and AI-controlled power electronics operating optimally for each user," in Proc. IEEE 29th International Symposium on Power Semiconductor Devices and ICs, May 2017, pp. 29 -32.

[6] K. Miyazaki, S. Abe, M. Tsukuda, I. Omura, K. Wada, M. Takamiya, and T. Sakurai, "General-purpose clocked gate driver IC with programmable 63-level drivability to optimize overshoot and energy loss in switching by a simulated annealing algorithm," IEEE Trans. on Industry Applications, vol. 53, issue 3, pp. 2350-2357, May-Jun. 2017.

[7] J. Dalton, J. Wang, H. Dymond, D. Liu, D. Pamunuwa, B. Stark, N. McNeill, and S. Hollis, "Shaping switching waveforms in a 650 V GaN FET bridge-leg using 6.7 GHz active gate drivers," in Proc. IEEE Appl. Power Electron. Conf. Expo., Mar. 2017, pp. 1983-1989.

[8] D. Colin, and N. Rouger "High speed digital optical signal transferforpower transistor gate driver applications," in Proc. IEEE 29th International Symposium on Power Semiconductor Devices and ICs, June 2017, pp. 37-40.

[9] H. Dymond, J. Wang, D. Liu, J. Dalton, N. McNeill, D. Pamunuwa, S. Hollis, and B. Stark, "A 6.7-GHz active gate driver for GaN FETs to combat overshoot, ringing, and EMI," IEEE Trans. on Power Electronics, vol. 33, no. 1, pp. 581-594, Jan. 2018.

[10] H. Obara, K. Wada, K. Miyazaki, M. Takamiya, and T. Sakurai, "Active gate control in half-bridge inverters using programmable gate driver ICs to improve both surge voltage and converter efficiency,"

IEEE Trans. on Industry Applications, vol. 54, issue 5, pp. 4603-4611, Mar. 2018.

[11] Y. Cheng, T. Mannen, K. Wada, K. Miyazaki, M. Takamiya, and T. Sakurai, "Optimization platform to find a switching pattern of digital active gate drive for full-bridge inverter circuit," i*n Proc. IEEE Energy Conversion Congress and Exposition*, Sep. 2018, pp. 6441-6443.

[12] Y. Cheng, T. Mannen, K. Wada, K. Miyazaki, M. Takamiya, T. Sakurai, "High-Speed searching of optimum switching pattern for digital active

gate grive circuit of full bridge inverter circuit," *in Proc. IEEE Appl. Power Electron. Conf. Expo.*, Mar. 2019, pp. 2740-2019.

[13] T. Sai, K. Miyazaki, H. Obara, T. Mannen, K. Wada, I. Omura, M. Takamiya, and T. Sakurai, "Load current and temperature dependent optimization of active gate driving vectors," *in Proc. IEEE Energy Conversion Congress and Exposition,* Sep. 2019, pp. 3292-3297.